Self-Assembly

DOI: 10.1002/ange.201006117

Supramolecularly Engineered Aggregation of a Dipolar Dye: Vesicular and Ribbonlike Architectures**

Shiki Yagai, Yujiro Nakano, Shu Seki, Atsushi Asano, Takashi Okubo, Takashi Isoshima, Takashi Karatsu, Akihide Kitamura, and Yoshihiro Kikkawa*

Functional dyes have gained increased attention because of the growing demands for low-cost and low-molecular-weight materials applicable to organic photovoltaic devices.[1] The major appealing features of these materials are the variable optical and electronic properties obtained through intermolecular electronic interactions.[2] Although this feature demands careful molecular design of the dyes, including taking their stacking arrangements into consideration for obtaining the desired optical and electronic properties, it offers a new possibility for tuning the properties by engineering specific noncovalent interactions.[1] Furthermore, tailoring of well-defined nanostructures by the bottom-up approach based on engineered noncovalent interactions[3] is emerging as a powerful strategy for increasing the number of potential applications of functional dyes. Dimension- and shape-controlled nanostructures consisting of optically and electronically active elements would show specific functions such as dimension-controlled transportation of excitons and charges.[4] Thus, simultaneous control over stacking arrangements and self-assembled architectures of functional dyes would produce organic optoelectronic materials with enhanced functionality. The stacking arrangements of various functional dyes have been controlled by modifying peripheral substituents,[5] host–guest complexation,[6] and hydrogen bonding.[7] For functional dyes having a strong dipole moment such as merocyanines, control of the stacking arrangement is particularly challenging because aggregation of this type of chromophore is susceptible to strong dipolar interactions, thus resulting in antiparallel face-to-face stacking arrangements (H-type aggregation).[8] The head-to-tail orientation (J-type aggregation) of merocyanine dyes[9] have been accomplished by Bosshard and co-workers[10] and Marks and co-workers[11] in vapor-phase deposited films, and by Würthner et al.[12] in a thermodynamically equilibrated system using hydrogen-bonding interactions. Herein, we report a novel supramolecular strategy to obtain J- and H-type aggregates of a dipolar dye using multiple hydrogen-bonding interactions, thereby leading to the formation of rationally organized vesicular and ribbonlike self-assembled architectures[13] with distinct optical and electronic properties (Scheme 1).

The merocyanine dye **1** bearing a barbituric acid (BA) group,[14] was synthesized as a hydrogen-bonding dipolar dye ($\mu = 10.9$ D). Previous studies have shown that the BA group is a useful supramolecular binding moiety that leads to the assembly of functional building blocks into well-defined nanostructures through self-complementary hydrogen bonds.[15] Self-aggregation of dye **1** proceeds through two intermolecular hydrogen-bonding interactions between each BA moiety, and subsequent hierarchical organization of the resulting hydrogen-bonded species through dipolar interactions (J-type aggregation). Upon addition of receptor **2**,[16] the BA group of **1** is capped, thereby shifting its aggregation mode through dipolar interactions (H-type aggregation).

The hydrogen-bonding pattern of **1** was studied by scanning tunneling microscopy (STM) at the liquid–solid interface. Figure 1a shows the STM image of **1** obtained at 1-phenyloctane/highly oriented pyrolytic graphite (HOPG) interface. Unidirectional lows of bright spots corresponding to the stilbene moiety of **1** were observed, indicating the formation of a linear hydrogen-bonding motif.[17] The periodic distance between the bright spots within the lows is (1.0±0.1) nm, which corresponds well to the hydrogen-bonding motif shown in Figure 1b which is among the various tapelike supramolecular structures found for the single crystals of barbituric acid derivatives (see Figure S1 in the Supporting Information).[18] The lows are separated alternately by the darker regions with a width of (1.0±0.1) nm (L1) and the darkest regions with a width of (1.5±0.1) nm (L2). The former regions correspond to linear hydrogen-bonded arrays of barbituric acid moieties, whereas the width of L2 is in good agreement with the length of dodecyl chains, suggesting the interdigitation of dodecyl chains between the hydrogen-bonded tapes (Figure 1b). One of the two alkyl chains of **1** is thus considered to be not physisorbed to the

[*] Prof. Dr. S. Yagai, Y. Nakano, Prof. Dr. T. Karatsu, Prof. Dr. A. Kitamura
Department of Applied Chemistry and Biotechnology
Graduate School of Engineering, Chiba University
1-33 Yayoi-cho, Inage-ku, Chiba 263-8522 (Japan)
Fax: (+81) 43-290-3039
E-mail: yagai@faculty.chiba-u.jp
Prof. Dr. T. Okubo
School of Science and Engineering, Kinki University (Japan)
Dr. T. Isoshima
Flucto-Order Functions Research Team, RIKEN Advanced Science Institute (RIKEN-ASI) (Japan)
Prof. Dr. S. Seki, A. Asano
Department of Applied Chemistry, Osaka University (Japan)
Dr. Y. Kikkawa
Photonics Research Institute, National Institute of Advanced Industrial Science and Technology (AIST) (Japan)

[**] This work was partially supported by the Ministry of Education, Science, Sports and Technology of Japan, Grant-in-Aid for Scientific Research (B) (No. 20350061).

Supporting information for this article is available on the WWW under http://dx.doi.org/10.1002/anie.201006117.

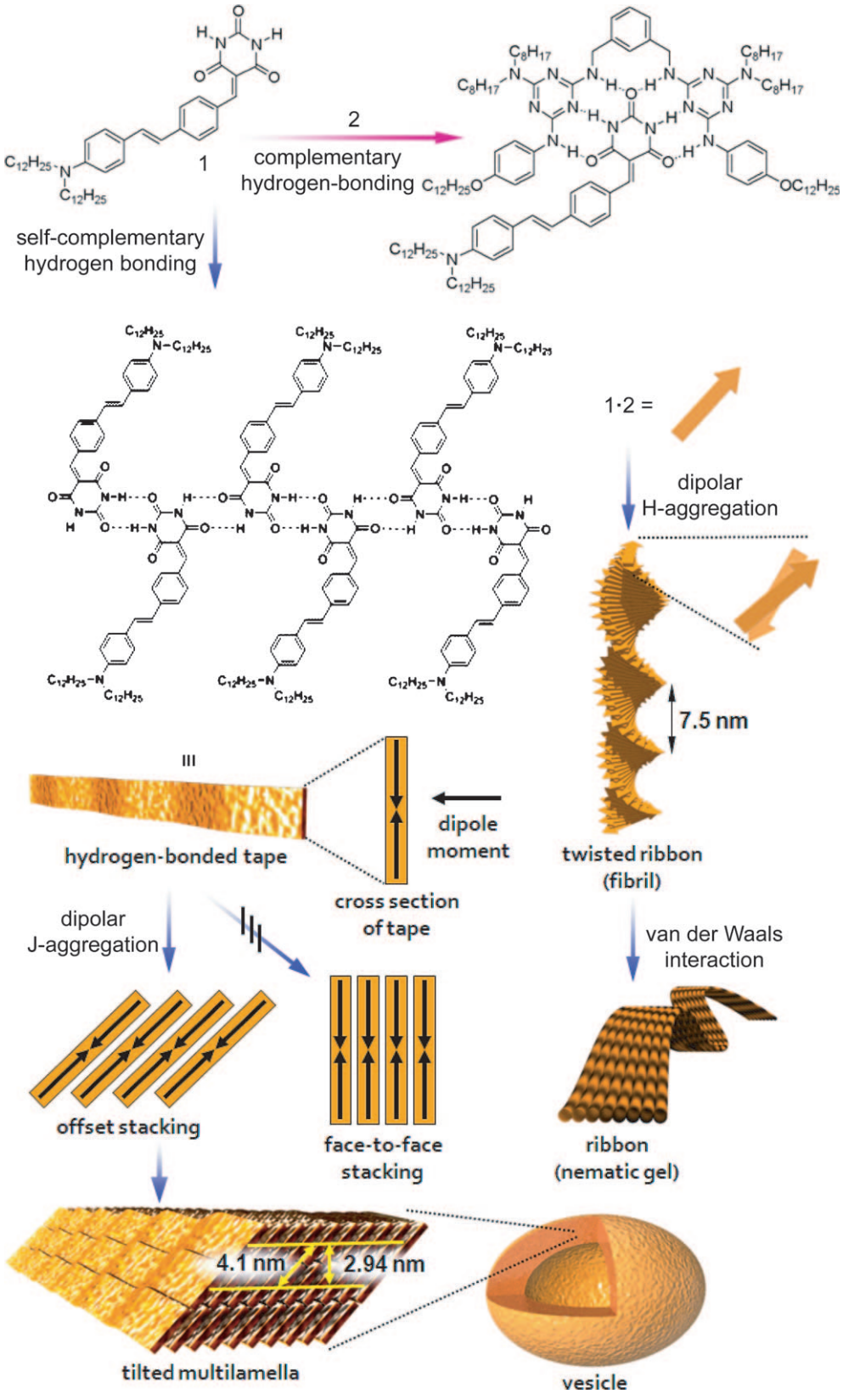

Scheme 1. Schematic representation of the self-organization process of **1** and subsequent J-aggregation into vesicles, and the formation of complex **1·2** and subsequent H-aggregation into ribbons.

surface. The interlayer spacing of hydrogen-bonded tapes (L3) is estimated to be (4.1 ± 0.1) nm.

In nonpolar solvents such as methylcyclohexane (MCH), hierarchical organization of the hydrogen-bonded tapes of **1** could take place, leading to a higher-order structure. **1** is poorly soluble in MCH ($c_{max} \approx 1 \times 10^{-5}$ M). The absorption spectrum of the $c = 1 \times 10^{-6}$ M solution exhibits vibronic transitions at $\lambda_{max} = 509$ and 541 nm (Figure 2a). Upon increasing the concentration to $c = 1 \times 10^{-5}$ M, a new band emerged in the red-shifted region around $\lambda = 600$ nm as a shoulder. The new band (J-band) disappeared upon heating to 90 °C (data not shown), suggesting that it originates from J-type aggregates of **1**. Notably, the observation of the J-band indicates that the hierarchical organization of the hydrogen-bonded tapes into two-dimensional sheets occurs through dipolar π–π stacking interactions because the distance between the neighboring stilbene moieties within the hydrogen-bonded tapes exceeds 10 Å.

Cooling of a hot (100 °C), homogeneous MCH solution of **1** ($c = 3 \times 10^{-5}$ M) to ambient temperatures results in a purple suspension. The absorption spectrum of the suspension shows an additional increase in the intensity of the J-band ($\lambda_{max} = 595$ nm, Figure 2a). Dynamic light scattering measurements demonstrated that the formation of particles having uniform hydrodynamic diameters (D_h) at around 600 nm (Figure 2b). Remarkably, scanning electron microscopy (SEM) of the particles revealed a coffee-bean-like ellipsoidal morphology (Figure 2c). The longer diameters of the ellipsoids are approximately 1 μm, which is larger than the D_h value in solution.

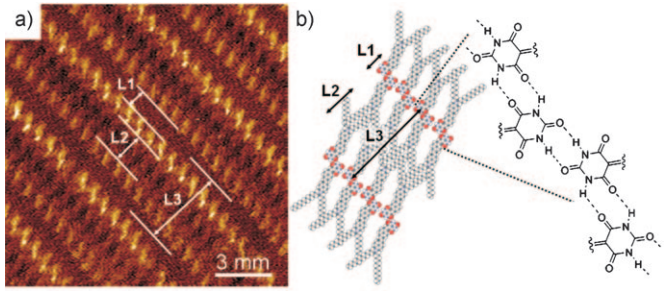

Figure 1. a) STM image of **1** at the 1-phenyloctane/HOPG interface. L1 and L2 show the widths of the barbituric acid and alkyl-tail arrays, respectively. L3 corresponds to the interlayer spacing of the hydrogen-bonded tapes. b) Proposed molecular arrangement of **1**.

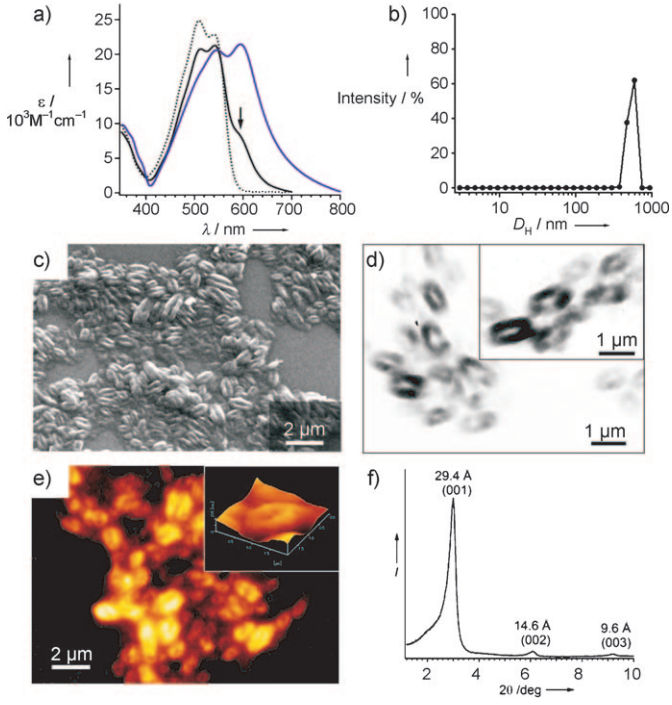

Figure 2. a) UV/Vis absorption spectra of homogeneous MCH solutions of **1** at concentrations of $c = 1 \times 10^{-6}$ M (dotted line) and $c = 1 \times 10^{-5}$ M (solid line), and its MCH suspension (purple line, $c = 3 \times 10^{-5}$ M) at 25 °C. Arrow indicates the J-band. b) Dynamic light scattering analysis of the MCH suspension ($c = 3 \times 10^{-5}$ M). c) SEM image of vesicular aggregates of **1** drop-cast from the MCH suspension onto a silicon substrate. d) TEM image of vesicular aggregates of **1** dip-coated from the MCH suspension onto carbon-coated TEM grid. The sample was sputtered by Ir/Pt at an angle of 45°. e) AFM image of vesicular aggregates of **1** drop-cast from the MCH suspension onto the HOPG surface. *z* scale = 200 nm. Inset: three-dimensional AFM image of a single vesicle. f) XRD pattern of vesicular aggregates of **1**.

The morphology of the ellipsoids was also visualized by transmission electron microscopy (TEM) after sputtering with Ir/Pt from an angle of 45° on a carbon-coated TEM grid. The image confirmed the presence of central concavity which shows a higher degree of penetration of electrons as a result of a low sputtering efficiency compared to that of the peripheral parts. Atomic force microscopy (AFM) revealed that the ellipsoids are between 100 and 200 nm in height with a concavity of 50 nm in depth (Figure 2e). On the basis of these microscopic observations, it is most likely that **1** self-assembles into vesicular (or erythrocytelike) aggregates in the solvent, which are deformed by the evaporation process.

X-ray diffraction of the vesicular aggregates exhibited explicit *d*-spacings at 29.4, 14.6, and 9.6 Å (Figure 2f), thus demonstrating that they are constructed by multilamellar organization of **1**. The interlayer spacing of 2.94 nm is shorter than that of the monolayer (L3) formed at liquid–solid interface (4.1 nm, Figure 1). Therefore, a tilted packing of the hydrogen-bonded tapes with respect to the lamellar normal by an angle of 44° is suggested for a higher-order organization of **1** (Scheme 1). The tilted packing is rationalized by observation of the J-band, which indicates an offset stacking of the tapes along to their short axes. Notably, the J-type aggregation of **1** is supramolecularly engineered by the formation of the antiparallel hydrogen-bonded tape which does not allow face-to-face stacking because of the unfavorable parallel orientation of the dipole moments (Scheme 1).

The addition of 0.2 equivalents of the barbituric acid receptor **2** to the MCH suspension of **1** results in the dissolution of vesicular aggregates, thus affording a transparent purple solution (Figure 3a). Interestingly, the UV/Vis spectrum of this solution retained the J-band ($\lambda_{max} = 585$ nm; Figure 3b). This observation implies that a small amount of **2** fragments the large vesicular aggregates into soluble J-type aggregates. Further addition of **2** resulted in an abrupt decrease in the intensity of the J-band and an increase in the intensity of a new absorption band at $\lambda_{max} = 514$ nm, exhibiting a prominent color change from purple to red (Figure 3a). The intensity of the new band was at a maximum when [**2**] = [**1**], which suggests a 1:1 complexation.

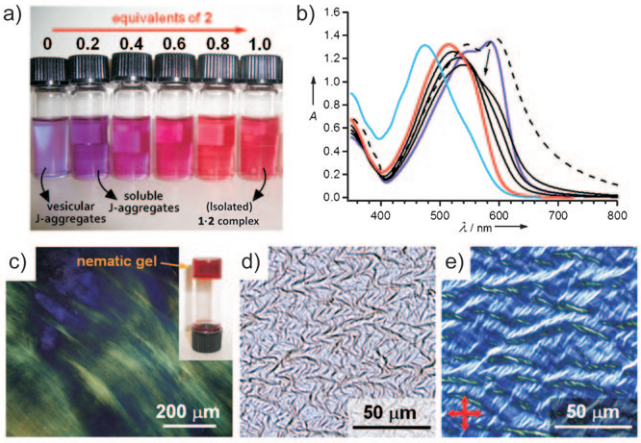

Figure 3. a) Color change of MCH solution of **1** ($c = 3 \times 10^{-5}$ M) upon increasing the equivalents of **2**. b) UV/Vis spectra of **1** ($c = 3 \times 10^{-5}$ M, $l = 1$ cm) with **2** in MCH. Arrow indicates the spectral change upon increasing the amount of **2** (purple to red lines; 0.2→1 equiv). The normalized spectrum at 0 equiv of **2** (-----; vesicular aggregates), and the normalized spectrum of **1·2** gel (blue line; $c = 2 \times 10^{-3}$ M) are shown. c) Polarized optical micrographic image of the **1·2** gel. Inset: picture of the gel in a vial. d) Optical and e) polarized optical microscopic images of the dried **1·2** gel.

The supramolecular species absorbing at $\lambda_{max} = 514$ nm is considered to be the hydrogen-bonded complex **1·2** that is free from dipolar aggregation because of its small red-shifted absorption maximum from that of the monomeric **1** in MCH ($\lambda_{max} = 509$ nm). The 5 nm red-shift would be a result of the polarizing effect by hydrogen-bonding interactions.[19] Additional association of this complex takes place upon increasing concentration, leading to gelation of the solutions at a concentration above $c = 2 \times 10^{-3}$ M and a blue-shift of the absorption maximum to $\lambda_{max} = 474$ nm (Figure 3b).[20] This observation illustrates that the packing arrangement of the merocyanine chromophores is shifted to an H-type arrangement. Polarized optical microscopic observation of the pristine gels showed a threadlike birefringent texture which is characteristic of the formation of nematic gels (Figure 3c).[21] Upon drying the gel between glass substrates, intertwined macroscopic fibers were generated and showed a maximum birefringence when they were aligned 45° relative to the polarizers (Figure 3d,e). This result suggests that π planes of the discotic complex are almost perpendicular to the long axis of the fibers.

AFM analysis of the dried gels of **1·2** showed flat ribbonlike nanostructures with widths of 50–200 nm lying on top of one another (Figure 4a). Notably, the individual ribbons are comprised of thinner fibrils arranged in side-by-side fashion (Figure 4b), consistent with the formation of the nematic gels. The body-to-body distance between neighboring fibrils is estimated by cross-sectional analysis to be 6 nm (Figure 4d; along i), which might correspond to the width of the fibrils. Remarkably, magnified phase imaging revealed that the elementary fibrils have either right- (*P*) or left-handed (*M*) helical structures with a regular pitch of 7.5 nm (Figure 4c and Figure 4d; along ii). Thus, it is strongly suggested that a rotational displacement of the discotic complex around the stacking axis occurs, leading to the formation of twisted ribbons (Scheme 1).[5a,22] The occurrence of the rotational displacement was supported by the electroabsorption spectroscopic analysis of the dried gels, which showed the presence of the transition to a lower-lying exciton state (at 550 nm), as well as the major transition to a higher-lying one (at 474 nm).[2] The transition to the theoretically forbidden lower-lying exciton state in the H-type aggregates originate from an imperfect H-type stacking arrangement with a rotational displacement (see Figure S5 in the Supporting Information).[23] Since the helical pitch corresponds to a 180° rotation of the discs, approximately 21 disks are involved in one pitch by assuming π–π stacking distance of 3.5 Å. Thus, the rotational angle between the neighboring disks is calculated roughly to be 9°.

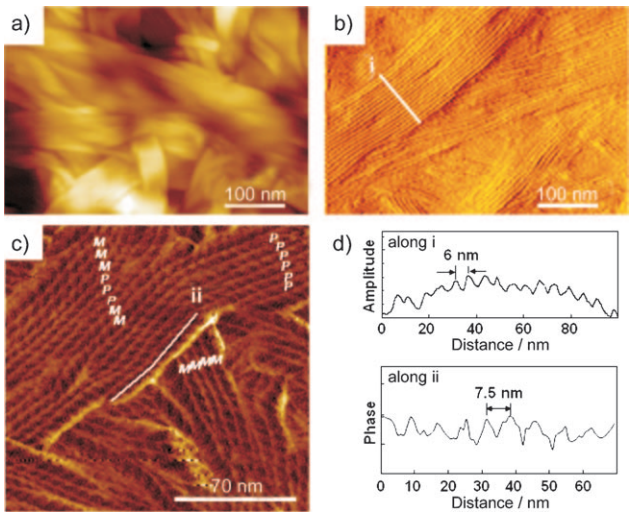

Figure 4. AFM images of dried MCH gel of **1·2** ($c = 2 \times 10^{-3}$ M). a) Height image, b) amplitude image, c) phase image, and d) cross-sectional profiles across the lines i and ii in b) and c), respectively. In c), the right- and left-handed twisted ribbons are designated by "*P*" and "*M*", respectively.

Molecular arrangement in semiconducting materials can have a significant impact on their charge-carrier mobilities and electrical conductivities.[24] We thus evaluated the mobilities of photogenerated charge carriers of self-assembled vesicular and ribbonlike aggregates by flash-photolysis time-resolved microwave conductivity measurement (FP/TRMC).[25] Upon excitation with a 355 nm laser pulse, the vesicular aggregates of **1** showed the maximum transient conductivity ($\phi\Sigma\mu$) of $4.4 \times 10^{-6}\,cm^2\,V^{-1}\,s^{-1}$, which is lower than the $\phi\Sigma\mu$ of $5.2 \times 10^{-6}\,cm^2\,V^{-1}\,s^{-1}$ observed for the ribbonlike aggregates of **1·2** (see Figure S6 in the Supporting Information). The photocarrier generation yields (ϕ) of the aggregates were determined to be 3.3×10^{-3} for **1** and 3.0×10^{-3} for **1·2** by photocurrent integration measurements (see Figure S7 in the Supporting Information). Thus, isotropic mobilities of photogenerated charge carriers within the aggregates ($\Sigma\mu$) were determined to be 1.3×10^{-3} and $1.7 \times 10^{-3}\,cm^2\,V^{-1}\,s^{-1}$ for **1** and **1·2**, respectively. Taking into account the one-dimensional columnar structure of the latter, charge-carrier transport is assumed to occur along the one-dimensional stacking axes directed randomly in the present case. Therefore, $\Sigma\mu$ of **1·2** was multiplied by a factor of three,[26] thus giving the one-dimensional mobility (μ_{1D}) of $5.1 \times 10^{-3}\,cm^2\,V^{-1}\,s^{-1}$. The higher mobility of the binary system is consistent with the efficient overlap of π-conjugated chromophores in the H-type aggregates.

Previous studies have shown that complementary multiple hydrogen-bonding interactions are a powerful tool for controlling either stacking arrangements[7b,d,g] or self-assembled structures[27] of functional dyes. Herein we have demonstrated that not only the aggregation mode of a dipolar dye but also the resulting self-assembled architectures can be rationally controlled by this supramolecular approach. As a result, optical and electronic properties of a single dye component can be tuned without any synthetic modifications. This study clearly demonstrates that supramolecularly engineered aggregation of functional dyes enhance the potential utility of these materials in optoelectronic applications.

Received: September 30, 2010
Published online: November 19, 2010

Keywords: dyes/pigments · hydrogen bonds · nanostructures · self-assembly · supramolecular chemistry

[1] "Supramolecular Dye Chemistry": *Topics in Current Chemistry, Vol. 258* (Ed.: F. Würthner), Springer, Berlin, **2005**.

[2] M. Kasha, H. R. Rawls, M. A. El-Bayoumi, *Pure Appl. Chem.* **1965**, *11*, 371 – 392.

[3] a) G. M. Whitesides, J. P. Mathias, C. T. Seto, *Science* **1991**, *254*, 1312 – 1319; b) J.-M. Lehn, *Supramolecular Chemistry: Concepts and Perspectives*, VCH, Weinheim, **1995**; c) D. N. Reinhoudt, M. Crego-Calama, *Science* **2002**, *295*, 2403 – 2407.

[4] a) E. W. Meijer, A. P. H. J. Schenning, *Nature* **2002**, *419*, 353 – 354; b) A. P. H. J. Schenning, E. W. Meijer, *Chem. Commun.* **2005**, 3245 – 3258; c) L. Zang, Y. Che, J. S. Moore, *Acc. Chem. Res.* **2009**, *41*, 1596 – 1608.

[5] a) A. Ajayaghosh, C. Vijayakumar, R. Varghese, S. J. George, *Angew. Chem.* **2006**, *118*, 470 – 474; *Angew. Chem. Int. Ed.* **2006**, *45*, 456 – 460; b) S. Yagai, M. Ishii, T. Karatsu, A. Kitamura, *Angew. Chem.* **2007**, *119*, 8151 – 8155; *Angew. Chem. Int. Ed.* **2007**, *46*, 8005 – 8009; c) S. Ghosh, X.-Q. Li, V. Stepanenko, F. Würthner, *Chem. Eur. J.* **2008**, *14*, 11343 – 11357.

[6] S. Gadde, E. K. Batchelor, J. P. Weiss, Y. Ling, A. E. Kaifer, *J. Am. Chem. Soc.* **2008**, *130*, 17114 – 17119.

[7] a) M. Shirakawa, S. Kawano, N. Fujita, K. Sada, S. Shinkai, *J. Org. Chem.* **2003**, *68*, 5037 – 5044; b) S. Yagai, M. Higashi, T. Karatsu, A. Kitamura, *Chem. Commun.* **2006**, 1500 – 1502; c) T. E. Kaiser, H. Wang, V. Stepanenko, F. Wurthner, *Angew. Chem.* **2007**, *119*, 5637 – 5640; *Angew. Chem. Int. Ed.* **2007**, *46*, 5541 – 5544; d) S. Yagai, T. Seki, T. Karatsu, A. Kitamura, F. Würthner, *Angew. Chem.* **2008**, *120*, 3415 – 3419; *Angew. Chem. Int. Ed.* **2008**, *47*, 3367 – 3371; e) Y. Sagara, T. Kato, *Angew. Chem.* **2008**, *120*, 5253 – 5256; *Angew. Chem. Int. Ed.* **2008**, *47*, 5175 – 5178; f) F. Würthner, C. Bauer, V. Stepanenko, S. Yagai, *Adv. Mater.* **2008**, *20*, 1695 – 1698; g) S. Yagai, S. Kubota, K. Unoike, T. Karatsu, A. Kitamura, *Chem. Commun.* **2008**, 4466 – 4468.

[8] a) F. Würthner, S. Yao, *Angew. Chem.* **2000**, *112*, 2054 – 2057; *Angew. Chem. Int. Ed.* **2000**, *39*, 1978 – 1981; b) F. Würthner, S. Yao, U. Beginn, *Angew. Chem.* **2003**, *115*, 3368 – 3371; *Angew. Chem. Int. Ed.* **2003**, *42*, 3247 – 3250; c) F. Würthner, K. Meerholz, *Chem. Eur. J.* **2010**, *16*, 9366 – 9373.

[9] J-aggregation of merocyanine dyes has been also achieved by the treatment of thin films of an amphiphilic merocyanines on SiO_2 electrode with the alkaline aqueous solution: K. Iriyama, F. Mizutani, M. Yoshimura, *Chem. Lett.* **1980**, 1399 – 1402.

[10] C. Cai, M. M. Bösch, Y. Tao, B. Müller, Z. Gan, A. Kündig, C. Bosshard, I. Liakatas, M. Jäger, P. Günter, *J. Am. Chem. Soc.* **1998**, *120*, 8563 – 8564.

[11] P. Zhu, H. Kang, A. Facchetti, G. Evmenenko, P. Dutta, T. J. Marks, *J. Am. Chem. Soc.* **2003**, *125*, 11496 – 11497.

[12] F. Würthner, J. Schmidt, M. Stolte, R. Wortmann, *Angew. Chem.* **2006**, *118*, 3926 – 3930; *Angew. Chem. Int. Ed.* **2006**, *45*, 3842 – 3846.

[13] Guest-induced transition between fibrous and vesicular nanostructures have been reported: a) A. Ajayaghosh, R. Varghese, V. K. Praveen, S. Mahesh, *Angew. Chem.* **2006**, *118*, 3339 – 3342; *Angew. Chem. Int. Ed.* **2006**, *45*, 3261 – 3264; b) J.-H. Ryu, H.-J. Kim, Z. Huang, E. Lee, M. Lee, *Angew. Chem.* **2006**, *118*, 5430 – 5433; *Angew. Chem. Int. Ed.* **2006**, *45*, 5304 – 5307; c) A. Ajayaghosh, P. Chithra, R. Varghese, *Angew. Chem.* **2007**, *119*, 234 – 237; *Angew. Chem. Int. Ed.* **2007**, *46*, 230 – 233; d) C. Wang, S. Yin, S. Chen, H. Xu, Z. Wang, X. Zhang, *Angew. Chem.* **2008**, *120*, 9189 – 9192; *Angew. Chem. Int. Ed.* **2008**, *47*, 9049 – 9052; e) A. Ajayaghosh, P. Chithra, R. Varghese, K. P. Divya, *Chem. Commun.* **2008**, 969 – 971.

[14] a) R. Ahuja, P. L. Caruso, D. Moebius, W. Paulus, H. Ringsdorf, G. Wildburg, *Angew. Chem.* **1993**, *105*, 1082 – 1085; *Angew. Chem. Int. Ed. Engl.* **1993**, *32*, 1033 – 1036; b) F. Würthner, S. Yao, *J. Org. Chem.* **2003**, *68*, 8943 – 8949.

[15] a) X. Huang, C. Li, S. Jiang, X. Wang, B. Zhang, M. Liu, *J. Am. Chem. Soc.* **2004**, *126*, 1322 – 1323; b) S. Yagai, S. Kubota, H. Saito, K. Unoike, T. Karatsu, A. Kitamura, A. Ajayaghosh, M. Kanesato, Y. Kikkawa, *J. Am. Chem. Soc.* **2009**, *131*, 5408 – 5410; c) S. Yagai, T. Kinoshita, Y. Kikkawa, T. Karatsu, A. Kitamura, Y. Honsho, S. Seki, *Chem. Eur. J.* **2009**, *15*, 9320 – 9324; d) C.-C. Chu, G. Raffy, D. Ray, A. D. Guerzo, B. Kauffmann, G. Wantz, L. Hirsch, D. M. Bassani, *J. Am. Chem. Soc.* **2010**, *132*, 12717 – 12723.

[16] a) S. K. Chang, A. D. Hamilton, *J. Am. Chem. Soc.* **1988**, *110*, 1318 – 1319; b) A. G. Bielejewska, C. E. Marjo, L. J. Prins, P. Timmerman, F. de Jong, D. N. Reinhoudt, *J. Am. Chem. Soc.* **2001**, *123*, 7518 – 7533.

[17] S. De Feyter, A. Miura, S. Yao, Z. Chen, F. Würthner, P. Jonkheijm, A. P. H. J. Schenning, E. W. Meijer, F. C. De Schryver, *Nano Lett.* **2005**, *5*, 77 – 81.

[18] J. C. MacDonald, G. M. Whitesides, *Chem. Rev.* **1994**, *94*, 2383 – 2420.

[19] J. Schmidt, R. Schmidt, F. Würthner, *J. Org. Chem.* **2008**, *73*, 6355 – 6362.

[20] The IR spectra of the gel and the vesicular aggregates also confirmed the formation of hydrogen bonds between **1** and **2** (see Figure S2 in the Supporting Information).

[21] a) H. von Berlepsch, C. Boettcher, L. Daehne, *J. Phys. Chem. B* **2000**, *104*, 8792 – 8799; b) J.-H. Ryu, M. Lee, *J. Am. Chem. Soc.* **2005**, *127*, 14170 – 14171.

[22] a) P. Jonkheijm, P. P. A. M. van-der-Schoot, A. P. H. J. Schenning, E. W. Meijer, *Science* **2006**, *313*, 80 – 83; b) A. Brizard, R. Oda, I. Huc, *Top. Curr. Chem.* **2005**, *256*, 167 – 218.

[23] U. Rösch, S. Yao, R. Wortmann, F. Würthner, *Angew. Chem.* **2006**, *118*, 7184 – 7188; *Angew. Chem. Int. Ed.* **2006**, *45*, 7026 – 7030.

[24] S. Prasanthkumar, A. Saeki, S. Seki, A. Ajayaghosh, *J. Am. Chem. Soc.* **2010**, *132*, 8866 – 8867.

[25] A. Acharya, S. Seki, A. Saeki, Y. Koizumi, S. Tagawa, *Chem. Phys. Lett.* **2005**, *404*, 356 – 360.

[26] a) F. C. Grozema, L. D. A. Siebbeles, J. M. Warman, S. Seki, S. Tagawa, U. Scherf, *Adv. Mater.* **2002**, *14*, 228 – 231; b) T. Amaya, S. Seki, T. Moriuchi, K. Nakamoto, T. Nakata, H. Sakane, A. Saeki, S. Tagawa, T. Hirao, *J. Am. Chem. Soc.* **2009**, *131*, 408 – 409.

[27] a) S. Yagai, T. Kinoshita, M. Higashi, K. Kishikawa, T. Nakanishi, T. Karatsu, A. Kitamura, *J. Am. Chem. Soc.* **2007**, *129*, 13277 – 13287; b) B. J. Jordan, Y. Ofir, D. Patra, S. T. Caldwell, A. Kennedy, S. Joubanian, G. Rabani, G. Cooke, V. M. Rotello, *Small* **2008**, *4*, 2074 – 2078; c) S. Yagai, S. Mahesh, Y. Kikkawa, K. Unoike, T. Karatsu, A. Kitamura, A. Ajayaghosh, *Angew. Chem.* **2008**, *120*, 4769 – 4772; *Angew. Chem. Int. Ed.* **2008**, *47*, 4691 – 4694; d) S. Yagai, S. Hamamura, H. Wang, V. Stepanenko, T. Seki, K. Unoike, Y. Kikkawa, T. Karatsu, A. Kitamura, F. Würthner, *Org. Biomol. Chem.* **2009**, *7*, 3926 – 3929; e) T. Tazawa, S. Yagai, Y. Kikkawa, T. Karatsu, A. Kitamura, A. Ajayaghosh, *Chem. Commun.* **2010**, *46*, 1076 – 1078; f) S. Yagai, H. Aonuma, Y. Kikkawa, S. Kubota, T. Karatsu, A. Kitamura, S. Mahesh, A. Ajayaghosh, *Chem. Eur. J.* **2010**, *16*, 8652 – 8661.

